Effects of Density and Gating of Delayed-Rectifier Potassium Channels on Resting Membrane Potential and its Fluctuations

S. Marom, H. Salman, V. Lyakhov, E. Braun

The Rappaport Faculty of Medicine and the Faculty of Physics, Technion-Israel Institute of Technology, Haifa 32000, Israel

Abstract. The aim of this study is to evaluate directly, using a reduced experimental system, the nature of interactions between voltage-gated potassium channels and the resting membrane potential. *Xenopus* oocytes were injected with various concentrations of cRNA coding for a delayed-rectifier potassium channel *Shaker*-IR. The effects of the density and kinetics of the expressed channels on resting membrane potential is explored in isolated (''inside-out'') patches. The channel density is given in terms of maximal conductance (G_{max}), measured from the maximal slope of the *I-V* curve under voltage clamp conditions. The capacitance of the experimental setup is approximately 1 pF. At high channel densities ($G_{max} > 10$ pA/mV) the mean membrane potential is stabilized at approximately −60 mV. This resting membrane potential is more than 35 mV positive to the reversal potential for potassium ions under the same experimental conditions. Analyses of voltage clamp experiments indicate that at high channel densities the mean membrane potential is determined by the rates of channel activation and deactivation, but is not affected by the rates involved in the process of slow (C-type) inactivation. In contrast, at lower channel densities membrane potential is very unstable, and its mean value and amplitude of fluctuations are strongly affected by the process of slow (C-type) inactivation.

Key words: Resting potential — Ion channel — Inactivation — Fluctuation — *Xenopus* oocyte

Introduction

Voltage-gated potassium channels participate in the stabilization of resting membrane potential in cells of many tissues. For example: the resting membrane potential in airway smooth muscle cells (Fleischmann, Washabau & Kotlikoff, 1993), dorsal root ganglion cells (Wang, Van den Berg & Ypey, 1994), and human retinal pigment epithelial cells (Hughes, Takahira & Segawa, 1995), was shown to be controlled by voltage-gated potassium channels. Although very diverse, many members of the voltage-gated potassium channels family share common gating properties (Hille, 1992; and references therein): Activation is usually fast and voltage-dependent, while inactivation is largely coupled to the activated state(s), occurs over a wide range of time scales, and is not strongly dependent on membrane potential. The coupling between voltage-dependent and voltage-independent reactions, taken together with the wide range of time scales involved, are important sources for modulations of the resting membrane potential. In this study, the nature of the interaction between voltage-gated potassium channels and the resting membrane potential is evaluated directly. The mean value of the resting membrane potential and its fluctuations are explored in a reduced system which allows control over the density and kinetics of ion channels. The reduced system is composed of a single potassium selective voltage-gated delayed-rectifier channel species, *Shaker*-IR (Hoshi, Zagotta & Aldrich, 1991), expressed at various densities in an isolated patch of *Xenopus* oocyte membrane (Fraser, Moon & Djamgoz, 1993). We show that the mean values and fluctuations of the membrane potential interact with the channel density and kinetics. At high channel densities, the mean value and fluctuations of resting membrane potential are sensitive to the activation-deactivation kinetics (i.e., Closed ⇔ Open), but are not sensitive to the inactivation kinetics (Open ⇔ Inactivated); in contrast, at lower densities the mean value and fluctuations of resting membrane potential are very sensitive to the rates of entry into and recovery from inactivation. The results are explained based on measured kinetics of the ion channel within the

framework of a simplified gating model, $C \Leftrightarrow O \Leftrightarrow I,$ where the $C \Leftrightarrow O$ transitions between the closed (C) and open (O) states are fast and voltage-dependent, and the $O \Leftrightarrow I$ transitions between the open (O) and inactivated (I) states are slow and voltage independent. The physiological significance of these findings is discussed.

Materials and Methods

EXPRESSION SYSTEM

Currents and voltages were measured from membranes of *Xenopus* oocytes that were injected with cRNA coding for a *Shaker* mutant, *Shaker*-IR. In this channel, positions 6–46 are deleted to remove the fast N-type inactivation (Hoshi, Zagotta & Aldrich, 1990; Hoshi, Zagotta & Aldrich, 1991), and a point mutation F425G is introduced (Goldstein & Miller, 1992). This particular mutant was chosen because it can be expressed at a very wide range of densities without apparent effects on its gating kinetics, and it demonstrates the typical fast-activating slowly-inactivating behavior of delayed-rectifier channels. Methods of DNA and cRNA preparation are standard and described elsewhere (Marom et al., 1993; Marom & Levitan, 1994). Oocytes were harvested from mature *Xenopus* females and dissociated in 2 mg/ml collagenase 1A (Sigma). Stage V-VI defolliculated cells were injected with 0.4–40 nl mRNA (~1 mg/ml). Injected cells were incubated at 18°C for up to seven days in frog Ringer's solution. The variability in expression of channels among different membranal regions of a single oocyte and between different oocytes enabled us to scan more than two decades of channel densities. The reported results are based on measurements from more than fifty oocytes originating from ten batches of injections.

ELECTROPHYSIOLOGY

Current clamp experiments were carried out in the detached patch configuration so that mean values of membrane potential and its fluctuations reflect processes that are inherent to the membrane itself, dissociated from intracellular effects. Pipettes were made from glass (#7052, Garner Glass, Claremont, CA) polished to 3–5 MΩ. All experiments were carried out at room temperature (22–25°C). The measured voltage was filtered at 10 KHz and sampled at 50 KHz. The bias current of the amplifier (Axopatch 200A, Axon Instruments, Foster City, CA) under current clamp is 0.3 pA and stable within and between experiments. Within the range of seal resistances that were used (5 to 55 GΩ, mean = 14.3 GΩ, n = 72) this bias current results in a mean hyperpolarizing shift of 1.5 to 16.5 mV (mean bias = −4.3 mV). The capacitance of the system (which is in fact the capacitance of the patch pipette itself) was reduced to ~1 pF by exposing the glass to the bath solution only at its tip. Unless mentioned otherwise, solutions for macro-patch recordings are as follows (concentrations in mM): external side −96 NaCl, 2 KCl, 1 CaCl$_2$, 1 MgCl$_2$, 10 HEPES, pH 7.5; cytoplasmic side − 95 KCl, 5 NaCl, 1 EGTA and 10 HEPES, pH 7.5. For experiments where potassium Nernst potential is the control parameter, the KCl in the external side solution in an outside-out patch configuration is modified, while NaCl is used to keep osmolarity constant. Each detached patch is tested for maximal voltage-gated potassium conductance (at the beginning of each experiment) and leak conductance (at the beginning and end of each experiment) in a voltage-clamp mode. Patches that demonstrated unstable seal resistance were excluded from the final analysis. For two electrode voltage clamp

(TEVC) recordings, a GeneClamp 500 amplifier (Axon Instruments, Foster City, CA) was used. Intracellular glass electrodes are filled with 2 M KCl, resulting in a resistance ranging from 0.5 to 2 MΩ. Bath solution in TEVC experiments is the same as pipette solution for macropatch experiments (see above). The TEVC was used as a complementary technique, allowing to span a wide range of channel densities in the kinetic analysis.

DATA ANALYSIS

Results are given in terms of a maximal potassium conductance, G_{max} (in pA/mV), which is measured directly from the slope of the *I-V* curve between +50 and +70 mV. G_{max} can be translated to number of channels in the patch based on a single-channel conductance of 13 pS (Yellen et al., 1991) and considering a system capacitance of ~1 pF. In these terms, a conductivity of 1 pA/mV corresponds to approximately one channel per µm^2 of membrane area. Rates of channel gating are inferred from kinetics of macropatch current relaxations in response to voltage perturbations. Activation and ''tail'' current traces, under voltage clamp conditions, were fitted to $I_K = A (1 - \exp[-t/\tau])^4$ and $I_K = A \exp[-4t/\tau]$, respectively (Hodgkin & Huxley, 1952). Rates were measured using a high potassium (30 mM) pipette solution (facing the outside of the membrane) to facilitate accuracy of measurements at voltages below −30 mV and to avoid potassium ion accumulation-effects. C-type inactivation rates were extracted from the relaxation of the current during depolarizing pulses, in fully activating membrane potential (>0 mV), and from the time course for recovery in double pulse experiments.

NUMERICAL SIMULATIONS

For numerical simulations of the three state model, $C \Leftrightarrow O \Leftrightarrow I,$ the probability of transition from one stat to the other is given by: $P = (1 - \exp[-k \, \Delta t])$, where k is the actual transition rate and Δt is a small (.25 msec) time step. The flipping between states is decided by picking a random number from a uniform distribution. The probability to move out from the open state (O) is calculated by the products of the probabilities to move into the closed (C) or inactive (I) states, $P = \exp[-(k_{oi} + k_{oc}) \, \Delta t]$. Once moved, the decision to which state to move is made by comparing another random number to the probability of inactivating given by $k_{oi}/(k_{oi} + k_{oc})$. $k_{co}(v)$ and $k_{oc}(v)$ values are taken from the functions derived from the results of voltage clamp experiments shown in the text. γ and δ are voltage independent rates for entry and recovery from inactivation, respectively. The channels are potassium selective, having a Nernst potential of −97 mV, and acting against a fixed leak conductance which is ten times larger than a single-channel conductivity. The leak Nernst potential was taken to be −9 mV. The capacitance of the system was taken to be 1 pF. Simulations were performed using Mathematica® (Wolfram Research, IL).

Results

THE BASIC OBSERVATIONS

As the maximal voltage-gated potassium conductance (G_{max}) increases, the membrane resting potential drops sharply to more hyperpolarized values (Fig. 1*A*) but appears to almost saturate around −60 mV (for $G_{max} > 10$ pA/mV, mean V_{rest} = −60.7 mV, SD = 2.6, n = 34). This resting membrane potential is more than 35 mV
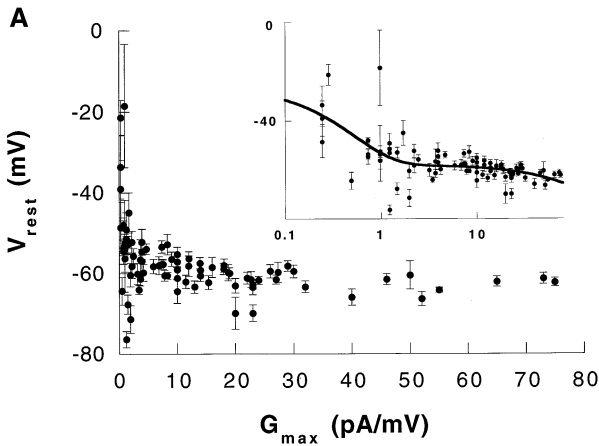
A

B

Fig. 1. (*a*) Effect of membrane channel density on the mean value of membrane potential. Density is given in terms of maximal slope conductance (G_{max}) calculated from current-voltage relations under voltage clamp conditions as described in Materials and Methods. Note the sharp decrement in mean membrane potential at low densities, followed by an almost stable value (~–60 mV) at higher densities. Error bars depict standard deviation. Each membrane potential was measured over periods of at least 2 min. Inset: The same data with logarithmic G_{max}. The data is fitted by a bi-exponential function with two characteristic G_{max} values (0.5 and 185). (*b*) Examples of voltage recordings at different channel densities. Maximal conductances are 0.24 pA/mV and 52 pA/mV at top and bottom traces, respectively. Each trace is 10-min long.
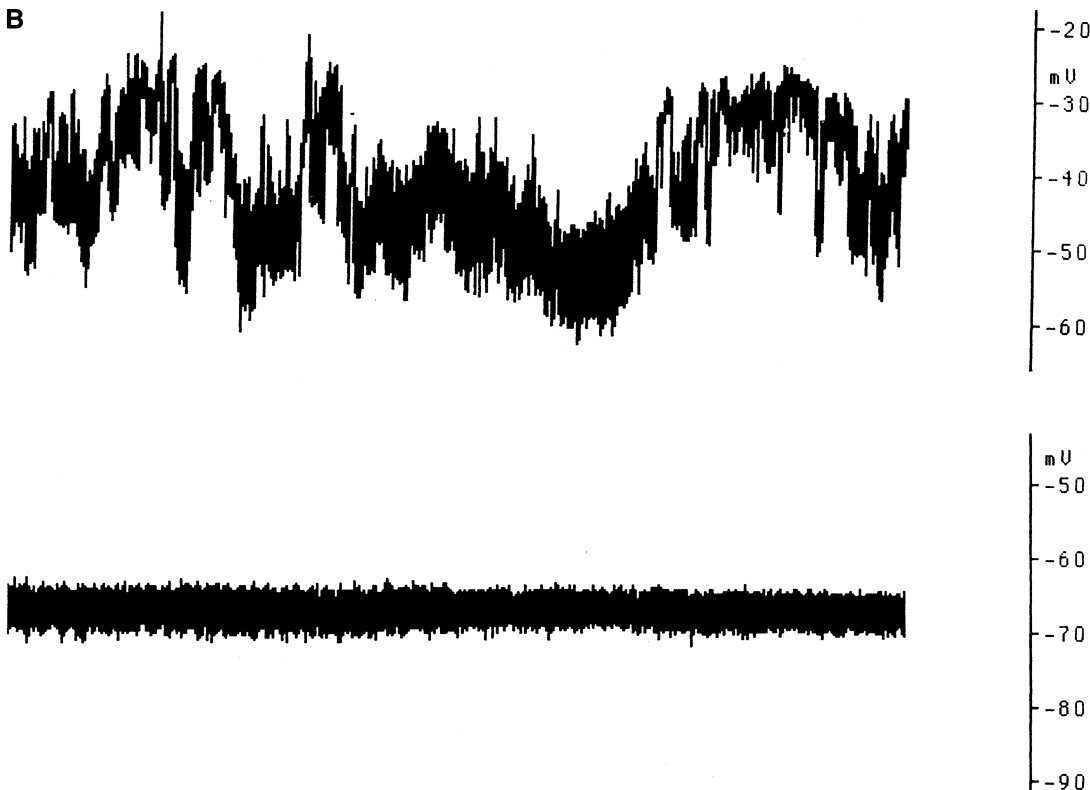
positive to the reversal potential for potassium ions under the same experimental conditions (measured from 'tail' currents, *data not shown*). The membrane potential of detached patches from uninjected oocytes ranges from –23 to +29.2 mV (mean = –7.72 mV, SD = 13.6, n = 18). Note from the error bars of Fig. 1*A,* and from the demonstration of raw data in Fig. 1*B,* that as potassium G_{max} increases, voltage traces become less noisy. These observations suggest that the density and kinetics of voltage gated potassium channels, in the model system studied here, are major factors that determine both the mean value and stability of the membrane potential. We show below that the mean value of the resting membrane potential and its fluctuations at high channel densities, are

a reflection of the fast activation-deactivation ($C \Leftrightarrow O$) kinetics. On the other hand, at lower channel densities, both mean and variance of membrane potential reflect the time scale separation between the slow inactivation ($O \Leftrightarrow I$) kinetics and the fast activation-deactivation kinetics. The characteristic value of channel density for switching between these two modes of behavior is determined by the leak conductance of the membrane.

EFFECT OF CHANNEL DENSITY AND KINETICS ON MEAN RESTING POTENTIAL

Since the value of the resting membrane potential in the reduced system is determined by the balance between the
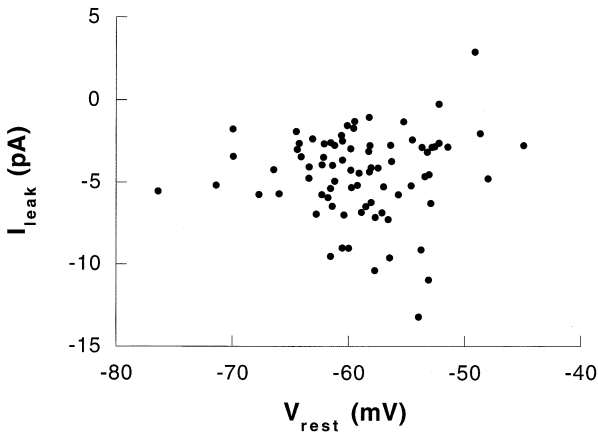
Fig. 2. Measured leak current *vs.* membrane potential: Measured leak currents for all the membrane patches shown in Fig. 1*A*, as a function of membrane potential. Leak current at resting membrane potential was extrapolated from the current responses to a series of hyperpolarizing pulses from −90 to −110 mV.

leak conductance and the voltage dependent potassium conductance, two possible mechanisms can account for the apparent saturation at −60 mV: (i) unique correlations between the spontaneous membrane potential and leak characteristics; (ii) effects of kinetics of the voltage gated ion channels. Figure 2 shows that a mechanism involving correlations between membrane potential and the leak characteristics is not likely; no significant correlation is found between V_{rest} and the leak current. This result implies that the source for the dependence of the resting membrane potential on the density of potassium channels is to be found in the gating machinery of the channels themselves. As shown below, the mechanism of membrane potential stabilization is dominated by a sharp change in the probability of the potassium channels to open above ~−60 mV.

Figure 3 summarizes voltage-clamp experiments that were designed for extraction of activation-deactivation rates and the probability for opening in an ensemble of many channels as a function of membrane potential. Note the gating behavior at the potential ranging from −60 to −40 mV (panels *c,d*): At more negative potentials, the chances for finding channels in the open state are extremely low. However, a sharp increase of the probability for opening is observed at potentials that are more positive to ~−60 mV. This result suggests that the resting membrane potential of our reduced system reflects the density of potassium channels only at potentials that are more positive to ~−60 mV. In agreement with this prediction, the value of the membrane resting potential is less sensitive to the potassium Nernst potential at values where the chances of the channels to open are reduced (Fig. 4).

In summary, the mean value of membrane resting potential interacts with the density of voltage gated po-

tassium channels: At low values of G_{max} (<10 pA/mV) a small change in G_{max} causes a marked change in resting membrane potential. This sensitivity is attenuated at higher values of G_{max}. The interaction seems to arise from channel gating properties and will be discussed later. We turn now to describe the membrane voltage fluctuations.

EFFECT OF CHANNEL DENSITY AND KINETICS ON
MEMBRANE POTENTIAL FLUCTUATIONS

As demonstrated in Fig. 1, in addition to the effect of channel density on the mean value of resting membrane potential, there is a marked effect on membrane potential fluctuations. Example of membrane potential amplitude histograms, of four 10-min sections and their sum, at a high channel density (~5000 channels/~1 μm^2 patch of membrane) are shown in Fig. 5*A*. The histogram is symmetric, can be described by a single Gaussian curve ($R > 0.95$), and reflects complex relations between rates for opening (α) and closing (β) of the channels as a function of membrane potential. Note, in Fig. 3*C,* the marked asymmetry around the voltage range between −50 to −60 mV. The asymmetry of relaxation rates suggests that there is no *a priori* reason for the membrane potential histogram to be symmetric and Gaussian. Although currently we have no mechanistic explanation for the symmetry, we note that when channel density goes to infinity, the histogram of membrane potential should collapse to a single point at exactly the potassium Nernst potential. Another intriguing point concerning the bell-shape of membrane potential histograms, is that over a very wide range of G_{max}, the variance deviates from the expected √N predicted by a simple Poisson process (*see* error bars in Fig. 1*A*). We interpret the relative independence of the variance in the number of channels at high channel densities to arise from the coupling to voltage: A fluctuation to higher membrane potential causes channels to open and thus shifts the membrane back to hyperpolarized potentials. A fluctuation to lower membrane potentials causes channels to close, shifting the membrane back to positive potentials. Overall, the distribution of membrane potential is constrained from both sides via membrane potential coupling. At these high channel densities, there are always sufficient numbers of noninactivated potassium channels to override the leak conductance, so that the fraction of channels in the inactivated state has no significant effect.

At low channel densities the behavior of the membrane potential is markedly different: the availability of every channel is important for balancing the leak conductance, and therefore all the time scales of channel gating affect the mean and distribution of the membrane potential. Accordingly, at low G_{max} the membrane potential cannot be described by a single Gaussian distri-
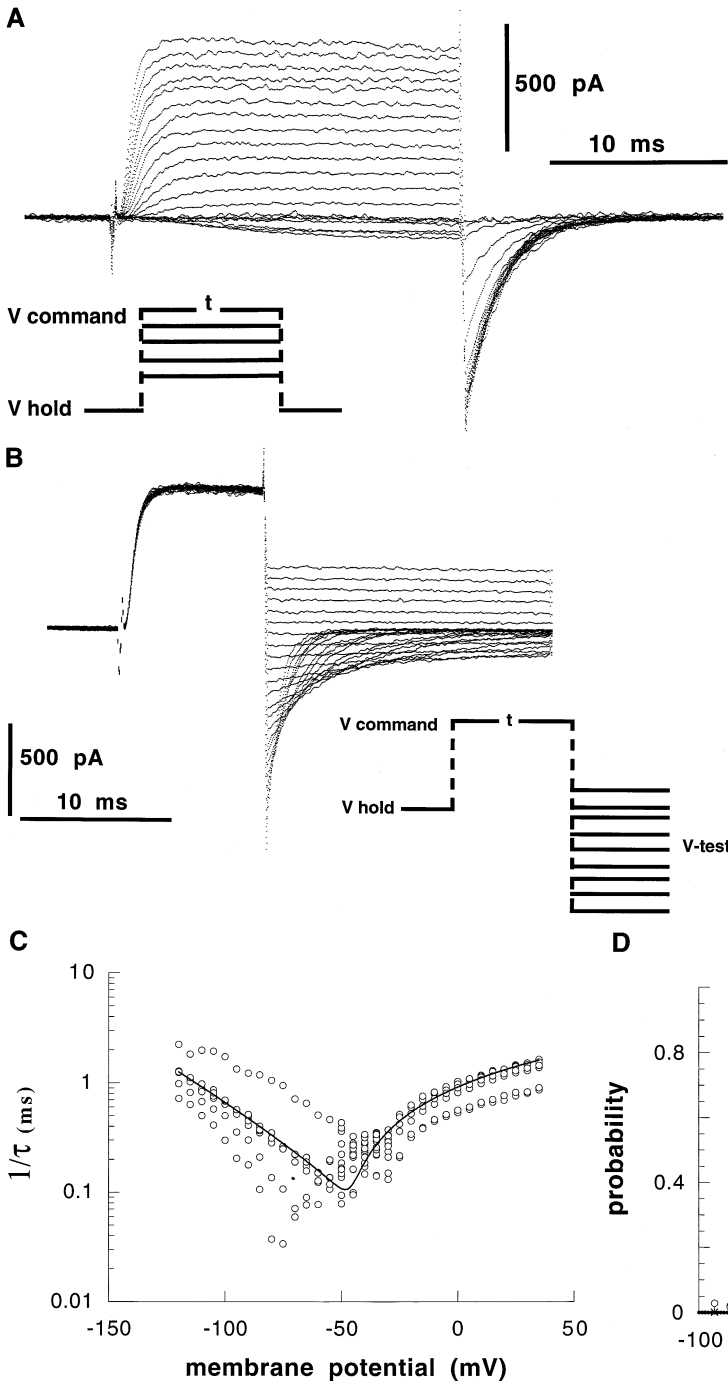
A

B

C

D

Fig. 3. Fast kinetics of the *Shaker*-IR: (*A*) Current responses to a family of depolarizing pulses from a −80 mV holding potential. Command voltages are from −50 to +40 mV in steps of 5 mV. The duration, *t,* of each pulse was 20 msec. Activation relaxations were fitted as described under Materials and Methods. Back extrapolations of tails were normalized and used for construction of maximal open probability *vs.* membrane potential (described in (*D*)). (*B*) Current relaxations at negative potentials were extracted from ''tail'' experiments where the membrane is depolarized to a fully activated potential (+40 mV) for 10 msec, followed by a hyperpolarizing period to different test membrane potentials (−120 to −30 mV in steps of 5 mV). Data, as in (*A*) and (*B*), of several experiments from three different cells, are used for the construction of (*C*), which shows relaxation times as a function of membrane potential. The data is fitted (continuous line) by:

$$\alpha = 0.03 \ (v + 46) \ / \ (1 - e^{-0.8 \ (v + 46)})$$
$$4\beta = -0.02 \ v \ e^{-0.023 \ (v + 148))}$$

(units in mV, msec). (*D*) Maximal open probability for *Shaker*-IR channels as a function of membrane voltage: The plot summarizes ten experiments that were conducted under voltage clamp conditions in two modes—detached patch recording configuration (×) and two electrode voltage clamp (O). The two techniques were applied in order to span a wide range of channel densities. No difference was detected between results from the two techniques. Dotted line depicts best fit to the data by $p = 1 \ / \ (1 + e^{-(v + 42)/4.8})$.

bution. As shown in Fig. 5*B,* where the behavior of a patch containing ~20 channels is described, the distribution is multimodal with a strong bias towards positive membrane potentials. This picture is very different from the histograms of high channel densities. The simplest explanation for the multimodal behavior is that C-type inactivation of the channels is involved (the characteristics of *Shaker*-IR inactivation are summarized in Fig. 6): At low channel densities, events of single-channel inac-

tivation affect all other available channels via a positive feedback loop. Each inactivation event causes a depolarization that increases the chances of more channels to open and inactivate. Thus, the probability that the membrane is depolarized for longer durations is increased. Such events can be resolved under current clamp conditions at high resolution as in Fig. 1*B* (upper trace). This phenomenon can in fact be thought of as an avalanche process in which the critical number of available chan-
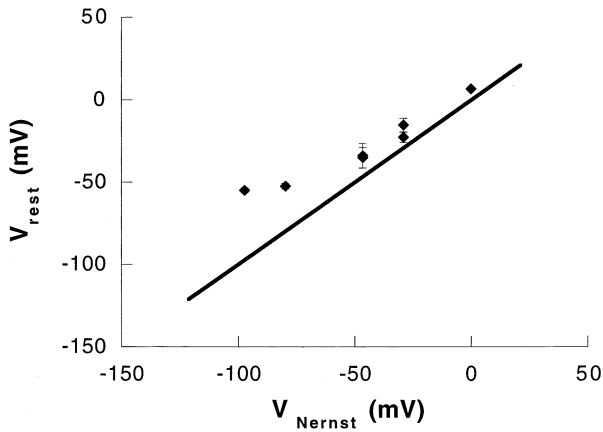
Fig. 4. The effect of potassium Nernst potential on mean membrane resting potential at high channel density: Solid line depicts the expected membrane potential assuming a pure potassium selective membrane. Note the disjoin between the expected and the measured membrane potentials at values that favor channel closing (compare to Fig. 3C). Measurements were performed after allowing complete relaxation from solution exchange. Error bars mark the fluctuations in membrane potential for at least two min of recording.

nels, below which the system will drift to positive potentials, is determined by the leak conductance and the rates of channel transitions.

SIMULATION STUDIES

A qualitative support for the above interpretation of the low G_{max} data was obtained by numerical simulations. Figure 7 shows the results of these simulations for 3, 20 and 200 channels/pF (equivalent to approximately 0.03, 0.2, and 2 pA/mV, respectively, in our reduced system).

Activation-deactivation and inactivation rates are directly extracted from data as in Figs. 3 and 6. Monte-Carlo simulations are performed as explained in Materials and Methods. The simulation study supports the idea that at low channel densities, the membrane resting potential distribution is expected to be multimodal, and that each peak at the distribution is correlated with a different number of available channels. An insight into the source of this behavior can be gained by imagining a system with total of N particles which are fluctuating between several states. To stabilize the system, n particles are required to be at a particular state. If $N \gg n$, as in the case of 200 channels (bottom trace and histogram), the microscopic fluctuations between the different states are insignificant from the system's stability point of view. The closer N and n are, the extreme of which is demonstrated in the simulation of three channels (upper trace and histogram), the microscopic transitions become more significant, all the transition rates become important, especially the slow transitions into and out of unavailable inactivated states.

Discussion

The conclusion from the results presented above is that the kinetics of voltage-gated ion channels affect the resting membrane potential and its fluctuations strongly. At high channel densities, the resting membrane potential is forced to a "threshold" potential for channel opening, and then adjusts itself according to the leak. This "threshold" potential can be predicted from the maximum of the second derivative of the probability-voltage curve for channel opening (Fig. 3). For the channels used in this study, the maximum value of the second
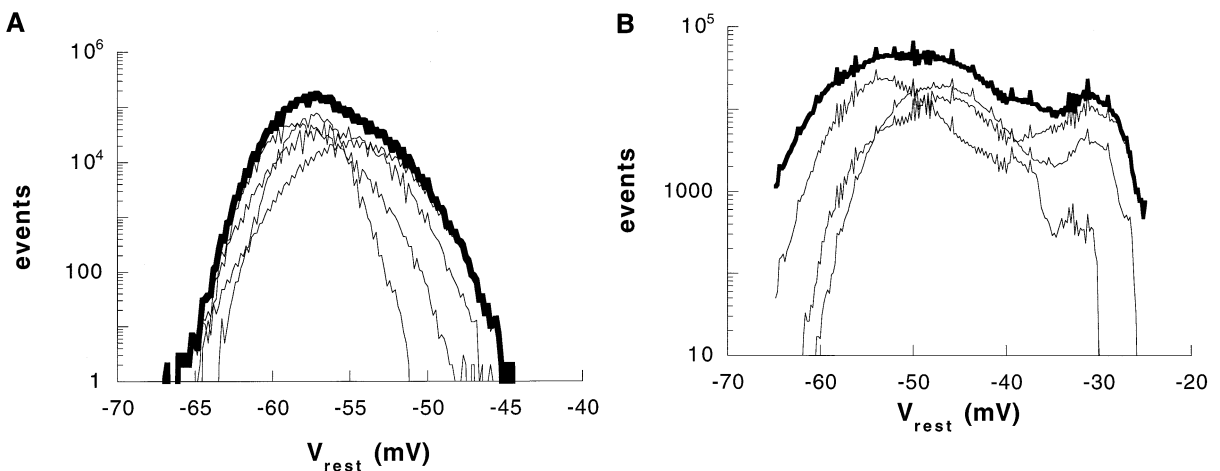

Fig. 5. (*a*) Amplitude histogram of membrane potential of a high density patch: $G_{max} = 52$ pA/mV. Thin lines depict separate 10-min sections from 40-min long amplitude histogram (thick line). Bin size: 175 μV. (*b*) Amplitude histogram of membrane potential of a low channel density patch. $G_{max} = 0.25$ pA/mV. Thin lines depict separate 10-min sections from the 30 min long amplitude histogram (thick line). Bin size: 175 μV.
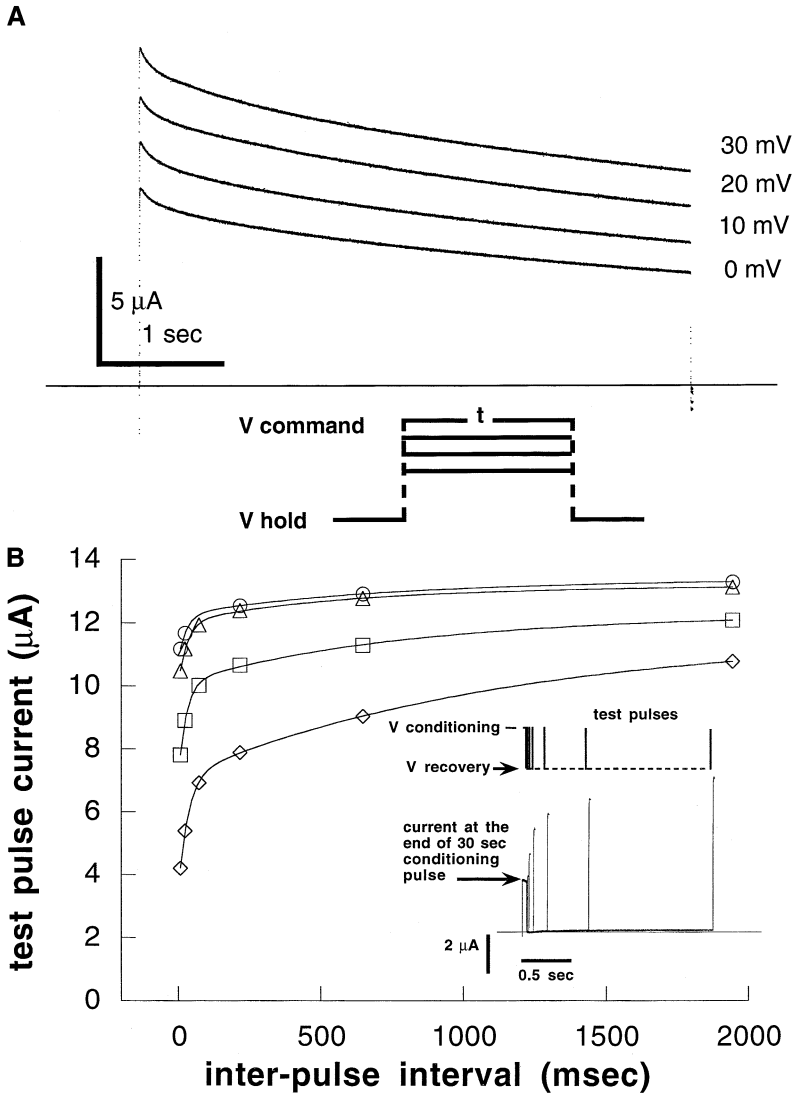
A

B

Fig. 6. C-type inactivation of the *Shaker*-IR. (*a*) Typical current responses to 4.5-sec long depolarizing pulses (from −80 mV to 0, 10, 20, and 30 mV). The time course of inactivation is, at least, bi-exponential (10.4 sec ± 0.77 sec, $n = 6$; and 171 msec ± 12 msec, $n = 6$). (*b*) Time course of recovery from C-type inactivation. Conditioning depolarization pulses of the following durations were used: 2 sec (circles), 3 sec (triangles), 10 sec (squares), and 30 sec (diamonds). Recovery follows a bi-exponential process: fast (29.8 msec ± 2.5 msec, $n = 5$) and slow (855 msec ± 220 msec, $n = 5$). Inset: example of current responses to a double-pulse voltage clamp experiment designed for estimation of recovery rates; each pair of pulses is composed of a long depolarizing pulse, followed by a shorter test pulse after indicated time interval at −80 mV; in the example shown in the inset, arrowhead depicts the residual current at the end of the 30-sec long pulse.

derivative is around −49 mV. This characteristic potential, when added to the contribution of the bias current under current clamp conditions (*see* Materials and Methods), approximates the measured value of −60 mV. At low channel densities, membrane resting potential is determined by a dynamic balance between the leak (''nongated'') conductance and the properties of voltage-gated conductances of the membrane. Accordingly, membrane potential distributions are much wider, and their mean is shifted to more positive values. Importantly, the voltage-gated channel that was chosen for this study belongs to the delayed-rectifier potassium channel family. Under natural conditions the value of resting potential and its fluctuations are probably affected also by other types of voltage-gated channels. It is suggested that the principles described in the present study can be accordingly scaled.

   The data of this study can be translated into realistic

channel densities, considering a system capacitance of ~1 pF. In these terms, a conductivity of 1 pA/mV corresponds to approximately 1 channel per μm^2 of membrane area. Fitting the data of Fig. 1 to an exponential function yields a conductance constant of 0.46 pA/mV which is equivalent to ~0.5 channels/μm^2. This characteristic potassium channel density is about one order of magnitude greater than the mean value of measured leak conductance in our system (0.07 pA/mV). In other words, 0.5 channels/μm^2 is a characteristic value beyond which the potential is stabilized around −60 mV with a symmetric distribution of fluctuations. Interestingly, the values of measured potassium channel densities in excitable membranes (Hille, 1992) range from 7/μm^2 (in the snail neuron) to ~1000/μm^2 (in the frog node), far beyond the minimum requirement for membrane stabilization, assuming a leak resistance of the order of 10 gigaohm. Potassium channel densities in these excitable
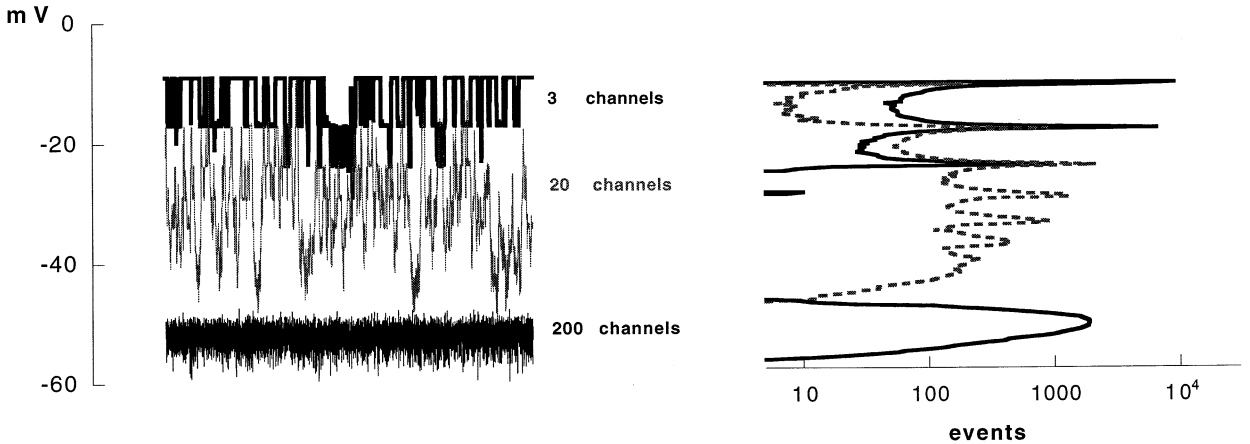
Fig. 7. Simulation studies (*see* Materials and Methods). The results of 25-sec long segments of numerical simulations to show that a multimodal membrane potential distribution at low channel densities can stem from a simple three state model of the form $C \Leftrightarrow O \Leftrightarrow I$. Simulation parameters: Single channel conductance was taken as 0.1 of leak conductance; α and β functions are described in Fig. 3C. For simplicity the many rates involved in inactivation were reduced to $\gamma = 0.005$ msec^{-1} and $\delta = 0.001$ msec^{-1}; these values approximate the fast relaxation of entry into, and the slow relaxation of recovery from C-type inactivation (Fig. 6). Left panel: traces of 25-sec duration. Right panel: amplitude histograms on a log scale.

systems might contribute to ensure a stable resting potential at values that are determined by the fast, and not the slow, channel kinetics. On the other hand, if the ratio between the rates of activation/deactivation and those that are involved in inactivation favors accumulation of channels in the inactive pool (DeCoursey, 1990; Aldrich, 1981; Marom & Levitan, 1994), the densities that will be required for membrane resting potential stabilization might be significantly higher.

Finally, we speculate that the resting potential of many types of excitable cells is at $\sim$−60 mV because many potassium channels demonstrate a characteristic knee at $\sim$−60 mV of their open probability-voltage curve (e.g., Hodgkin & Huxley, 1952; Hoshi & Aldrich, 1988; Stühmer et al., 1989; Kirsch, et al., 1991; Perozo et al., 1992).

References

Aldrich, R.W. 1981. Inactivation of voltage-gated delayed potassium current in molluscan neurons. *Biophys. J.* **36:**519–532

DeCoursey, T.E. 1990. State-dependent inactivation of K$^+$ currents in rat type II alveolar epithelial cells. *J. Gen. Physiol.* **95:**617–646

Fleischmann, B.K., Washabau, R.J., Kotlikoff, M.I. 1993. Control of resting membrane potential by delayed rectifier potassium currents in ferret airway smooth muscle cells. *J. Physiol.* **469:**625–638

Fraser, S.P., Moon, C., Djamgoz, M.B.A. 1993. Electrophysiology of *Xenopus* oocytes: an expression system in molecular neurobiology. *In:* Electrophysiology, A Practical Approach. D.I. Wallis, editor. pp. 65–86. Oxford University Press, Oxford

Goldstein, S.A.N., Miller, C. 1992. A point mutation in Shaker K$^+$ channel changes its charybdotoxin binding site from low to high affinity. *Biophys. J.* **62:**5–7

Hodgkin, A.L., Huxley, A.F. 1952. A quantitative description of membrane current and its application to conduction and excitation in nerve. *J. Physiol.* **117:**500–544

Hille, B. 1992. Ionic channels of excitable membranes. Sinauer Associates, MA

Hoshi, T., Aldrich, R.W. 1988. Voltage-dependent K$^+$ currents and underlying single K$^+$ channels in pheochromocytoma cells. *J. Gen. Physiol.* **91:**73–106

Hoshi, T., Zagotta, W.N., Aldrich, R.W. 1990. Biophysical and molecular mechanisms of *Shaker* potassium channel inactivation. *Science.* **250:**533–538

Hoshi, T., Zagotta, W.N., Aldrich, R.W. 1991. Two types of inactivation in *Shaker* K$^+$ channels: effects of alterations in the carboxy-terminal region. *Neuron.* **7(4):**547–556

Hughes, B.A., Takahira, M., Segawa, Y. 1995. An outwardly rectifying K$^+$ current active near resting potential in human retinal pigment epithelial cells. *Am. J. Physiol.* **269:**C179–C187

Kirsch, G.E., Drewe, J.A., Verma, S., Brown, A.M., Joho, R.H. 1991. Electrophysiological characterization of a new member of the RCK family of rat brain K$^+$ channels. *FEBS Lett.* **278(1):**55–60

Marom, S., Goldstein, S.A.N., Kupper, J., Levitan, I.B. 1993. Mechanism and modulation of inactivation of the Kv3 potassium channel. *Receptors & Channels.* **1:**81–88

Marom, S., Levitan, I.B. 1994. State-dependent inactivation of the Kv3 potassium channel. *Biophys. J.* **67:**579–589

Perozo, E., Papazian, D.M., Stefani, E., Bezanilla, F. 1992. Gating currents in *Shaker* K$^+$ channels. Implications for activation and inactivation models. *Biophys. J.* **62:**160–171

Stühmer, W., Ruppersberg, J.P., Schröter, K.H., Sakmann, B., Stocker, M., Giese, K.P., Perschke, A., Baumann, A., Pongs, O. 1989. Molecular basis of functional diversity of voltage-gated potassium channels in mammalian brain. *The EMBO J.* **8(11):**3235–3244

Wang, Z., Van den Berg, R.J., Ypey, D.L. 1994. Resting membrane potentials and excitability at different regions of rat dorsal root ganglion neurons in culture. *Neuroscience* **60:**245–254

Yellen, G., Jurman, M.E., Abramson, T., MacKinnon, R. 1991. Mutations affecting internal TEA blockade identify the probable pore-forming region of a K$^+$ channel. *Science* **251:**939–942